EXCLI Journal 2014;13:19-27 – ISSN 1611-2156
Received: November 04, 2013, accepted: January 14, 2014, published: January 29, 2014

Original article:

AUTOMATIC QUANTITATIVE ANALYSIS OF MORPHOLOGY OF APOPTOTIC HL-60 CELLS

Yahui Liu[1], Wang Lin[1], Xu Yang[1], Weizi Liang[1], Jun Zhang[1], Maobin Meng[2], John R. Rice[3], Yu Sa[1*], Yuanming Feng[1,2,3*]

[1] Department of Biomedical Engineering, Tianjin University, Tianjin, China
[2] Department of Radiation Oncology, Tianjin Medical University Cancer Institute and Hospital, Tianjin China
[3] Department of Radiation Oncology, East Carolina University, Greenville, NC/USA

* Corresponding authors: Yu Sa, sayu@tju.edu.cn; Yuanming Feng, fengyu@ecu.edu

ABSTRACT

Morphological identification is a widespread procedure to assess the presence of apoptosis by visual inspection of the morphological characteristics or the fluorescence images. The procedure is lengthy and results are observer dependent. A quantitative automatic analysis is objective and would greatly help the routine work. We developed an image processing and segmentation method which combined the Otsu thresholding and morphological operators for apoptosis study. An automatic determination method of apoptotic stages of HL-60 cells with fluorescence images was developed. Comparison was made between normal cells, early apoptotic cells and late apoptotic cells about their geometric parameters which were defined to describe the features of cell morphology. The results demonstrated that the parameters we chose are very representative of the morphological characteristics of apoptotic cells. Significant differences exist between the cells in different stages, and automatic quantification of the differences can be achieved.

Keywords: cell morphology, quantitative analysis, apoptosis

INTRODUCTION

Apoptosis occurs in an orderly fashion with morphological events including cell shrinkage, the degradation of DNA, orderly condensation of the nucleus, and the production of membrane "blebbs" which are phagocytosed by surrounding cells. This sequence of events was termed "apoptosis" by Kerr et al.(1972). Study of apoptosis has attracted significant attention in cancer research and anticancer technology development in recent years. Much research has been conducted with visual inspection of fluorescent images of stained cells under microscopes (Van Cruchten and van den Broeck, 2002; Kalinichenko and Matveeva, 2008). The morphological identification of apoptotic cells in fluorescent microscopic images is currently the most widely used method, but it is ambiguous because of the limited qualitative description. The technique is also labor intensive, time-consuming, and the accuracy of the final results ultimately depends on the skill and experience of the observer. It has been challenged by practices in analyzing large amount of cells to obtain statistically meaningful results(Hoyt et al., 1997). An automatic approach is therefore needed in the study of morphological changes associated with cell apoptosis.

EXCLI Journal 2014;13:19-27 – ISSN 1611-2156
Received: November 04, 2013, accepted: January 14, 2014, published: January 29, 2014

Most of the published studies focused on segmentation approaches (Gurcan et al. 2006; Dorini et al., 2007; Cseke, 1992) and did not include the extraction or analysis of geometric parameters and quantification of apoptotic cell morphology. Our research aims at quantitatively analyzing the morphological changes in different apoptotic stages of HL-60 cells. For this purpose, we have implemented an image processing and segmentation method, defined adequate parameters and an automatic method for morphological measurement which are presented in the next section followed with experimental results and discussion.

MATERIALS AND METHODS

Image acquisition

Brief exposure of cultured cells to hydrogen peroxide (H_2O_2) can induce cellular death that proceeds via an apoptotic pathway (Kovar et al., 1997). In this study, human leukemia cells (HL-60) were cultured at 37 °C in a humidified 5 % CO_2 atmosphere in the media ofRPMI1640 (Life Technologies, New York) with 10 % heat-inactivated fetal bovine serum(FBS, Life Technologies) and treated with 1.5 mM $H_2O_2$for 24 h. They were stained with Hoechst33342 and AnnexinV-FITC/PI(Life Technologies) to determine the apoptosis stage. Cell nuclei marked by PI are identified as late apoptosis in this study (including nerocrosis) which are shown in red color in the fluorescent images. AnnexinV can be conjugated to a variety of fluorochromes, and binds to "flipped" Phosphatidylserine (PS) residues on extracellular membrane leaflet of apoptotic cells. Hoechst33342 is a highly permeable DNA binding dye that enters cells and labels their chromatin regardless of their viability state(Telford et al., 2011). In other words, normal cells are stained by Hoechst33342 (Hoechst33342+, AnnexinV-, PI-), early apoptotic cells are stained by AnnexinV but not PI (AnnexinV+, PI-), and only late apoptotic cells are stained by PI (PI+).

The stained cells in the experiments were photographed in a light channel (Figure 1a) and three fluorescent channels (Figure 2a) with an inverted fluorescence microscope (IVFM, IX71, Olympus). The experiments were repeated three times independently. The image resolution is 1367×1038 and the calibration setting for the cell images is 32×magnification, which gives 0.3225 μm/pixel.

Segmentation

Automatic and quantitative analysis of cellular morphological changes in fluorescent microscopic images requires the development of algorithms for segmenting the cells individually and for quantifying their shape parameters accurately without manual interaction (Angulo and Schaack, 2008). Thresholding becomes an effective tool of separating objects from backgrounds when their gray levels are substantially different. The morphological method is also widely used in both subsequent processing steps and initial segmentation (Meijering, 2012). The algorithm used in our method combines these methods to achieve faster segmentation for images with different features.

Ideal images for the automatic segmentation should contain compact cells in a uniform background. Raw images obtained in experiments contain noise from samples, the microscope light channel and three fluorescent channels, and need to be preprocessed. The image enhancement algorithm we used to facilitate segmentation is described as follows (Nasonov and Krylov, 2012). For light microscope images, the morphological opening method was first applied to correct non-uniform illumination. Then we used a 5×5 window median filtering combined with grayscale stretch to improve the image quality of light channel and each fluorescent channel of microscopic images. Median filtering is useful for reducing random noise and periodic patterns (Weber and Albrecht, 1997; Huang et al., 1979), and grayscale stretch can expand the dynamic range of a region of interest. The background noise and the interference of

EXCLI Journal 2014;13:19-27 – ISSN 1611-2156
Received: November 04, 2013, accepted: January 14, 2014, published: January 29, 2014

other channels were excluded after the pre-processing (Figure 1b).

The classical clustering-based Otsu threshold segmentation algorithm is an automatic method to find the threshold which can divide the given image into foreground and background through maximizing the between-class variance (Poletti et al., 2012; Xu et al., 2011). Suppose that pixels in a given image are represented in m gray levels, the ith level has n_i pixels, and the total number of pixels is $N=\sum_{i=1}^{m} n_i$. The probability of occurrence of each level in the given image is $p_i=n_i/N$, and the mean value is $\mu=\sum_{i=1}^{m} ip_i$. Pixels are now divided into two classes C0={1~k} and C1={k+1~m} with probability of $\omega_0=\sum_{i=1}^{k} p_i=\omega(k)$ and $\omega_1=\sum_{i=k+1}^{m} p_i=1-\omega(k)$. The mean level of each class is

$$\mu_0=\sum_{i=1}^{k}\frac{ip_i}{\omega_0}=\frac{\mu(k)}{\omega(k)} \quad and \quad \mu_1=\sum_{i=k+1}^{m}\frac{ip_i}{\omega_1}=\frac{\mu-\mu(k)}{1-\omega(k)} \quad (1)$$

To reach the largest difference as expressed in Eq. 2, the variance between the two classes should reach the maximum. The threshold is given in Eq. 3.

$$\sigma^2(k)=\omega_0(\mu_0-\mu)^2+\omega_1(\mu_1-\mu)^2=\omega_0\omega_1(\mu_1-\mu_0)^2=\frac{[\mu\omega(k)-\mu(k)]^2}{\omega(k)[1-\omega(k)]} \quad (2)$$

$$k^*=arg\max_k \sigma^2(k) \quad (3)$$

The Otsu method is the least time-consuming segmentation method suitable for the process of a large amount of images, yet very sensitive to noise and the target size. To alleviate the noise impact to the segmented results, we used robust pre-processing methods as described above to enhance the image.

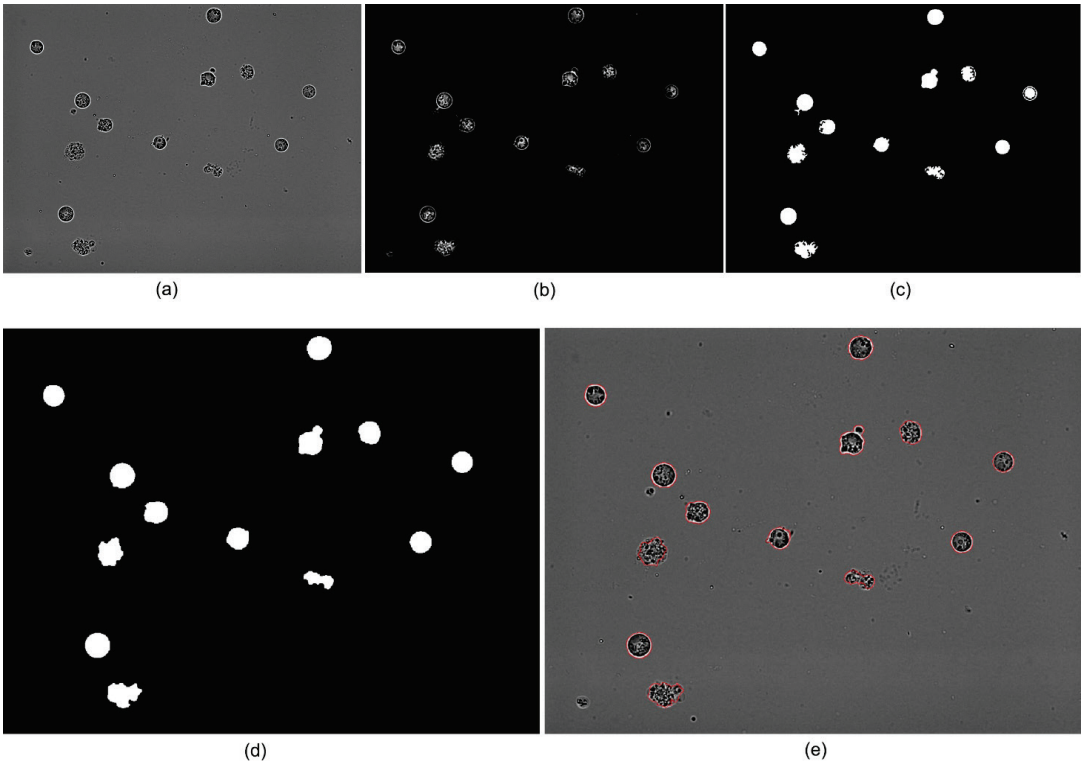

Figure 1: Light channel images and the segmentation. (a) original image; (b) after pre-processing; (c) segmentation with the Otsu method; (d) after processing with dilation and erosion operators; (e) outlined cells on the original image

EXCLI Journal 2014;13:19-27 – ISSN 1611-2156
Received: November 04, 2013, accepted: January 14, 2014, published: January 29, 2014

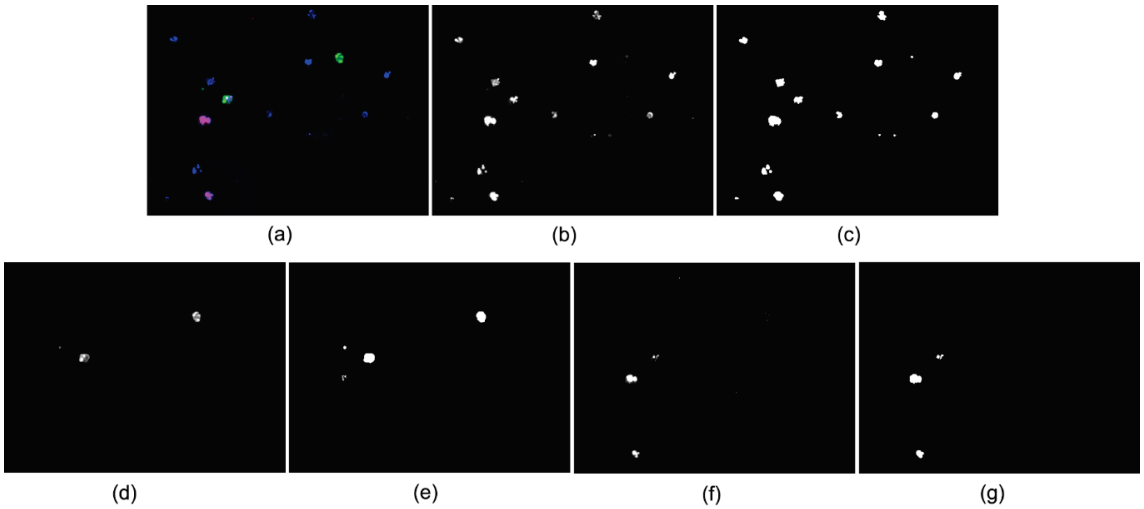

Figure 2: Fluorescent image segmentation. (a) original image; (b) B channel image; (c) B channel image after segmentation; (d) G channel image; (e) G channel image after segmentation; (f) R channel image; (g) R channel image after segmentation

The dilation and erosion operators were repeated in turn as post-seg processing to deal with some small regions and holes in the binarized image (Yua et al. 2009; Di Ruberto et al., 2002). The small objects whose areas were smaller than the averaged size of the objects were removed. The objects on the board were also deleted in case they were not complete (Gonzalez et al., 2009). Figure1d and 1e show the final segmentation result of a light channel image, and Figure 2b-g show images of each channel, as well as their segmentation results.

Parameter extraction and statistical analysis

The cells in light channel images were matched to corresponding cell nuclei based on their location according to a pre-calibrated distance from a cell center to its nucleus center (less than 20 pixels in our study). For each cell, we programmed to search for a nucleus satisfying this condition and identified it as the corresponding nucleus. After this step, the algorithm was designed to determine apoptotic stage of cells, i.e., normal cells (Hoechst33342+, AnnexinV-, PI-), early apoptotic cells (AnnexinV+, PI-) and late apoptotic cells (PI+) according to the staining results of corresponding cell nuclei. This procedure aims at counting cells in each stage. As shown in Figure 3e-g, cell nuclei of each stage were divided and shown in separated images. Figure 3h shows the cell stage determination results (3 normal cell nuclei, 1 late apoptotic cell nucleus and 1 early apoptotic nucleus), which is consistent with that of visual examination. More figures of light channel images and the corresponding fluorescent images with segmented contours are shown in the supplementary material.

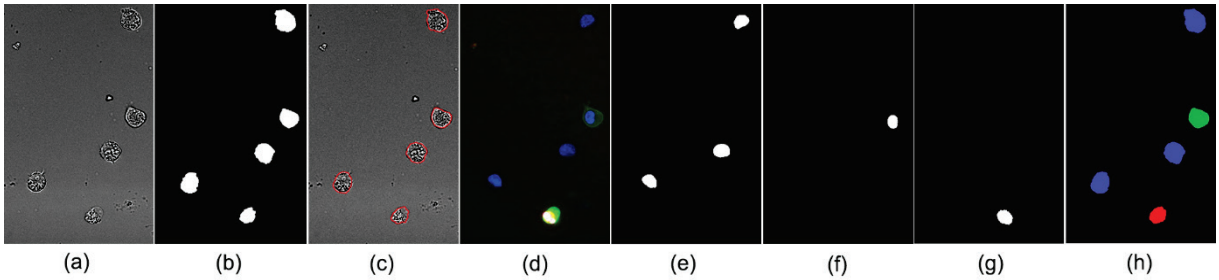

Figure 3: Cell stage determination. (a) original light channel image; (b) segmented light channel image; (c) outlined cells on the original light channel image; (d) original fluorescent image; (e) normal cell nuclei; (f) early apoptotic cell nuclei; (g) late apoptotic cell nuclei; (h) labeled cells, normal cells are labeled in blue, an early apoptotic cell is labeled in green, and a late apoptotic cell is labeled in red.

EXCLI Journal 2014;13:19-27 – ISSN 1611-2156
Received: November 04, 2013, accepted: January 14, 2014, published: January 29, 2014

Several parameters were chosen and defined for the description of HL-60 cells (Table 1), including basic and widely used geometric parameters such as cell Area and Perimeter. Shape Factor is also known as an important indicator of cell morphology. The closer to a circular shape the object is, the nearer to 1 the Shape Factor will be. It is related to "cell shrink" or the smoothness of the cell edge. Center Distance between nucleus and cytoplasm was used as a reflection of chromatin margination. We also proposed Smoothness Index (defined as the perimeter of the object divided by the perimeter of an equivalent circle) and Number of Pit Points of the cell membrane as characteristic parameters to represent the extent of "cell blebbing". The first 5 parameters listed in Table 1were also used to describe the morphology of the cell nuclei.

For the calculation of Number of Pit Points of cell membrane, the convex hull of each cell membrane was generated. Then the concave area of this cell membrane was found out by removing the cell area from the whole area of the convex hull. Points on the boundary of the concave area reaching the local minimum distances to the centroid of the cell were marked as pit points. Other parameters were calculated according to their definition. All of the algorithms are programmed with MATLAB R2012a.

A one-way analysis of variance (one-way ANOVA) test was used in the statistical analysis of the parameters characterizing cell morphology change between the three cell stages (SigmaPlot12.0, San Jose, California).

Table 1: Parameters for description of apoptotic cell morphology[1]

Parameter	Definition
Area	area enclosed by cell edge
Perimeter	length of cell edge
Shape Factor	$4\pi A/C^2$,C: perimeter, A: area. It shows the extent of irregularity.
Roundness	$\sqrt{A/\pi}/R$, A: area, R: mean radius. It shows the degree of deviation of an object's boundary from a circle.
Ovality	d_{max}/d_{min}, d_{max}: maximum diameter, d_{min}: minimum diameter. It describes oval shape characteristics.
Shape Irregular Index	radius of equivalent perimeter/radius of equivalent area. It describes the extent of irregularity.
Smoothness Index	perimeter/perimeter of equivalent circle. It describes the extent of "cell blebbing".
Number of Pit Points	number of points on the boundary reaching local minima of distance to the centroid. It describes the smoothness of cell edge.
Center Distance between nucleus and cytoplasm	distance between centre of nucleus and centre of cell. It describes the extent of nucleus margination.
RNP	$A_n/A_p = A_n/A_c - A_n$, A_c: cell area, A_p: cytoplasm area, A_n: nucleus area. It describes the relative size of cytoplasm and nucleus, nucleus condensation.

[1]The unit of Area is pixel^2 (=0.3225 μm×0.3225 μm), the unit of Perimeter and Center Distance between nucleus and cytoplasm is pixel (=0.3225 μm).

EXCLI Journal 2014;13:19-27 – ISSN 1611-2156
Received: November 04, 2013, accepted: January 14, 2014, published: January 29, 2014

RESULTS AND DISCUSSION

Figure 4 shows the representative cells for each stage (normal, early apoptosis and late apoptosis) segmented with the algorithm. The morphological parameters (listed in Table 1) of (a), (b), (c) and (d) in Figure 4 were calculated for pre-analysis.

The ones with large variance that can articulate the attribute clearly were chosen for the quantitative analysis (Table 2). The parameters of "Number of Pit Points" of the blebbing apoptotic cells and the late apoptotic cells are larger than those of the normal cells and the apoptotic cells of non-blebbing. The Smoothness Index of the blebbing apoptotic cells is the largest, revealing the situation of "cell blebbing".

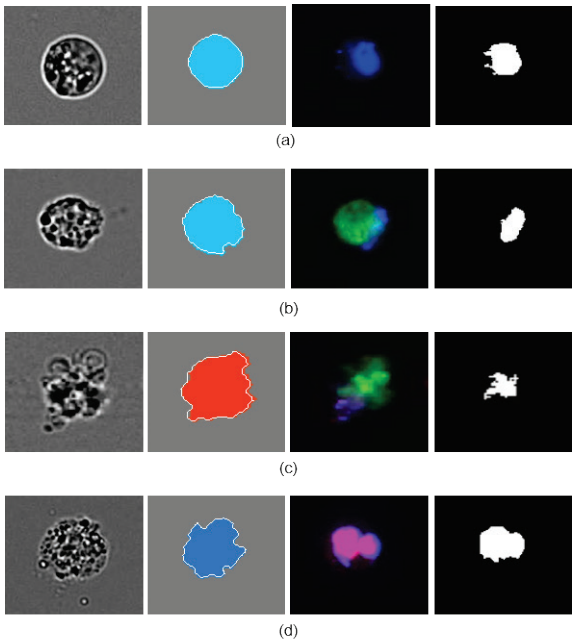

Figure 4: Boundary extraction of cell membrane and nucleus. (a) Normal cell; (b) Early apoptotic cell; (c) Early apoptotic cell with blebbing; (d) Late apoptotic cell

Table 2: Parameters of the cells in Figure 4

Parameter	(a)	(b)	(c)	(d)
Perimeter of membrane	189	194	350	213
Area of nucleus	825	412	255	470
Perimeter of nucleus	109	121	87	147
Shape Factor of membrane	0.9202	0.6594	0.4903	0.8503
Roundness of membrane	0.5412	0.4581	0.3950	0.5202
Ovality of membrane	1.0076	1.7717	2.3872	1.0832
Smoothness Index of membrane	1.8476	2.1827	2.531	1.9221
Shape Factor of nucleus	0.8685	0.3479	0.4199	0.2722
Roundness of nucleus	0.5257	0.3327	0.3656	0.2943
Ovality of nucleus	1.0076	1.253	1.1811	1.0832
Number of Pit Points of membrane	2	4	8	3
Center Distance between nucleus and cytoplasm	6.07	15.82	19.29	9.89

Table 3: Classification results of the three groups

Group	Total cells	Classification			Accuracy Ratio[1]
		Normal	Early apoptosis	Late apoptosis	
1	190	89	40	61	93 %
2	204	87	52	65	91 %
3	195	91	42	62	90 %

[1] Accuracy Ratio is calculated as the number of cells correctly classified divided by the total number of cells

Results of the statistical analysis for the three groups of the parameters obtained from the three independent experiments and characterizing the morphology of the HL-60 cells in three stages are summarized in Table 4. After calculating the mean value and standard deviation (SD) of each parameter, one-way ANOVA tests for the parameters between the three cell stages were conducted. Parameters such as Shape Factor and Roundness of membrane as well as those of nucleus share the same phenomenen as shown in Figure 5a for Shape Factor of membrane, with mean values of normal cells significantly larger than those of apoptotic cells. This reveals that normal cells are closer to circles, while early apoptotic cell membranes have more irregular shapes because of "blebbing" and "shrinking". On the contrary, Perimeter,Ovality, Smoothness Index, Number of Pit Points of membranes, Area, Perimeter, Ovality, Smoothness Index of nucleus and Center Distance between nucleus and cytoplasm show the differences between the three stages as illustrated in Figure 5b for Ovality of nucleus. Ovality of nucleus varies greatly between cells in different stages, from which we can see that nucleus shapes of early apoptotic cells are closer to oval than those of cells in the other two stages. One-way ANOVA test results for the Center Distance between nucleus and cytoplasm show that there is a statistically significant difference (P=0.023), which reveals that the margination of cell nucleus can be reflected by the change of this parameter. Its mean value for early apoptotic cells is larger, because chromatin margination usually happens in this stage. In each group, SDs of the parameters of normal cells are the smallest, and those of early apoptotic cells are the largest, revealing that normal cells have relatively homogeneous morphology while apoptotic ones vary greatly.

Table 4: Statistical results of the parameters[1]

Parameter	normal	early apoptosis	late apoptosis
Perimeter of membrane	224 ± 6.3740	282 ± 7.2040	267 ± 8.5171
Area of nucleus	1209 ± 144.2331	1690 ± 74.9438	1564 ± 21.7538
Perimeter of nucleus	152 ± 9.4006	188 ± 5.4200	176 ± 7.3532
Shape Factor of membrane	0.8611 ± 0.0016	0.7031 ± 0.0042	0.7279 ± 0.0046
Roundness of membrane	0.5219 ± 0.0023	0.4711 ± 0.0020	0.4796 ± 0.0020
Ovality of membrane	1.0754 ± 0.0127	1.2782 ± 0.0157	1.2293 ± 0.0166
Smoothness Index of membrane	1.9222 ± 0.0092	2.1437 ± 0.0158	2.0960 ± 0.0156
Shape Factor of nucleus	0.6512 ± 0.0175	0.6067 ± 0.0077	0.6537 ± 0.0098
Roundness of nucleus	0.4584 ± 0.0172	0.4330 ± 0.0049	0.4485 ± 0.0026
Ovality of nucleus	1.0833 ± 0.0147	1.2611 ± 0.0235	1.2191 ± 0.0048
Number of Pit Points of membrane	1.43 ± 0.3010	5.59 ± 0.1758	4.36 ± 0.731
Center Distance between nucleus and cytoplasm	7.49 ± 0.2807	9.29 ± 0.8667	8.35 ± 0.3548

[1] In the form of mean ± SD from the three groups with cell numbers listed in Table 3 for each group. $p<0.05$ in one-way ANOVA test between cell stages for each parameter, which indicates there is a significant difference between cells in different stages for each parameter.

EXCLI Journal 2014;13:19-27 – ISSN 1611-2156
Received: November 04, 2013, accepted: January 14, 2014, published: January 29, 2014

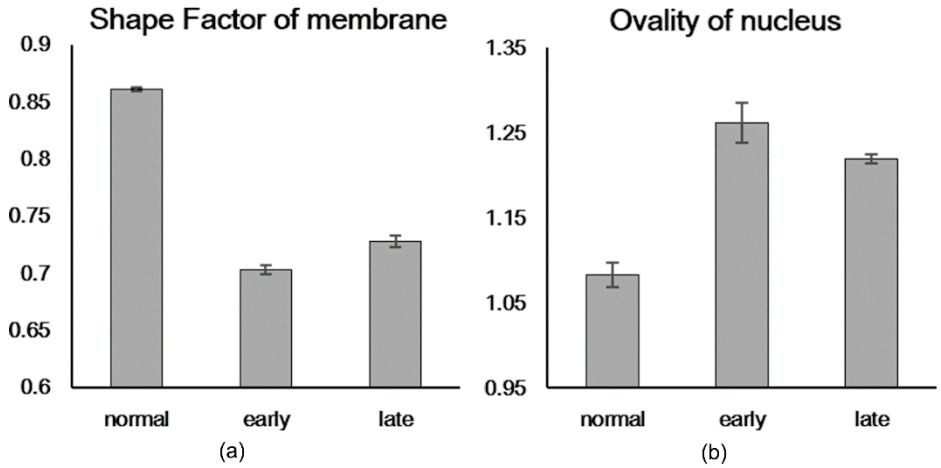

Figure 5: Statistical results of the parameters in different cell stage. Each column represents a parameter's mean and standard deviation (SD) for the cells in each stage from the three independent experimental studies. (a) Shape Factor of membrane of normal cells is the largest among the 3 stages ($p<0.05$ in one-way ANOVA test). (b) Ovality of nucleus of early apoptotic cells is significantly larger than that of normal cells and late apoptotic cells ($p<0.05$ in one-way ANOVA test).

CONCLUSION

The experimental results demonstrate that the image processing algorithm presented in this manuscript can effectively extract morphological features of cells from fluorescent microscopic images and achieve accurate staging results. It is less time-consuming as compared to manual contour tracing and parameter extraction. The chosen parameters are representative and can describe the characteristics of cell images precisely. Most of the parameters show great differences between the three stages, which indicates that the morphological differences between normal cells and apoptotic cells can be detected quantitatively with the automatic method.

There are still challenges in developing methods that are applicable and effective for a wide range of cell images with various morphological cellular features and different image characteristics. In addition, further study is required to find out if the parameters chosen in this study can also be applied to other cell types in quantitatively describing apoptosis morphology.

Acknowledgments: The authors acknowledge the support of NSFC (grants #81171342, #81041107, #31000784 and #81201754).

Conflict of Interests: The authors declare that there is no conflict of interests regarding the publication of this article.

REFERENCES

Angulo J, Schaack B. Morphological-based adaptive segmentation and quantification of cell assays in high content screening. In: Proceeding of 5th IEEE International Symposium on Biomedical Imaging: From Nano to Macro (pp 360-3). Paris: IEEE, 2008.

Cseke I. A fast segmentation scheme for white blood cell images[C]. In: 11th IAPR International Conference on Pattern Recognition, 1992. Conference C: Image, Speech and Signal Analysis, Proceedings (pp 530-3). IEEE, 1992.

Di Ruberto C, Dempster A, Khan S. Analysis of infected blood cell images using morphological operators. ImageVis Comput2002;20:133-46.

Dorini LB, Minetto R, Leite NJ. White blood cell segmentation using morphological operators and scale-space analysis[C]. In: XX Brazilian Symposium on Computer Graphics and Image Processing, 2007 (pp 294-304). SIBGRAPI 2007. IEEE, 2007.

Gonzalez RC, Woods RE, Eddins SL. Digital image processing using MATLAB (chapt. 7). Knoxville: Gatesmark Publishing, 2009.

Gurcan MN, Pan T, Shimada H, Saltz J. Image analysis for neuroblastoma classification: segmentation of cell nuclei[C]. In: Engineering in Medicine and Biology Society 2006. EMBS'06. 28th Annual International Conference of the IEEE (pp 4844-7). IEEE, 2006.

Hoyt KR, Gallagher AJ, Hastings TG. Characterization of hydrogen peroxide toxicity in cultured rat forebrain neurons. Neurochem Res1997;22:333-40.

Huang TS, Yang GJ, Tang GY. A fast two-dimensional median filtering algorithm. IEEE Trans Acoust Speech Sign Process1979;27:13-8.

Kalinichenko SG, Matveeva NY. Morphological characteristics of apoptosis and its significance in neurogenesis. Neurosci Behav Physiol 2008;38:333-44.

Kerr J, Currie A, Wyllie A. Apoptosis: a basic biological phenomenon with wide-ranging implications in tissue kinetics. Brit J Cancer 1972;26:239-57.

Kovar J, Stunz LL, Stewart BC. Direct evidence that iron deprivation induces apoptosis in murine lymphoma 38C13. Pathobiology 1997;65:61-8.

Meijering E. Cell segmentation: 50 years down the road. IEEE Signal Proc Mag 2012;29:140-5.

Nasonov V, Krylov AS. Edge quality metrics for image enhancement. Patt Recogn Image Anal 2012; 22:346-53.

Poletti E, Zappelli F, Ruggeri A. A review of thresholding strategies applied to human chromosome segmentation. Comput Meth Prog Bio 2012; 108:679-88.

Telford WG, Komoriya A, Packard BZ, Bagwell CB. Multiparametric analysis of apoptosis by flow cytometry. In: Hawley TS, Hawley RG (eds.): Flow cytometry protocols, 3rd ed. (pp 203-28). New York, NY: Human Press, 2011. (Methods in Molecular Biology, Vol. 699).

Van Cruchten S, van den Broeck W. Morphological and biochemical aspects of apoptosis, oncosis and necrosis. Anat Histol Embryol 2002;31:214-23.

Weber I, Albrecht R. Image processing for combined bright-field and reflection interference contrast video microscopy. Comput Meth Prog Bio 1997;53:113-8.

Xu X, Xu S, Jin L. Characteristic analysis of Otsu threshold and its applications. Pattern Recogn Lett 2011;32:956-61.

Yua D, Phamb TD, Zhou X. Analysis and recognition of touching cell images based on morphological structures. Comput Biol Med 2009;39:27-39.